

Considering light-matter interactions in the Friedmann equations

V. Vavryčuk

The Czech Academy of Sciences

Boční II 1401, 141 00 Praha 4

vv@ig.cas.cz

ABSTRACT

Recent observations indicate that the Universe is not transparent but partially opaque due to absorption of light by ambient cosmic dust. This implies that the Friedmann equations valid for the transparent universe must be modified for the opaque universe. The paper studies a scenario when the opacity steeply rises with redshift. In this case, the light-matter interactions become important, because cosmic opacity produces radiation pressure that counterbalances gravitational forces. The presented theoretical model assumes the Universe expanding according to the standard FLRW metric but with the scale factor $a(t)$ depending on both types of forces: gravity as well as radiation pressure. The modified Friedmann equations predicts a cyclic expansion/contraction evolution of the Universe within a limited range of scale factors with no initial singularity. The model avoids dark energy and removes some other tensions of the standard cosmological model. The paper demonstrates that considering light-matter interactions in cosmic dynamics is crucial and can lead to new cosmological models essentially different from the standard Λ CDM model. This emphasizes necessity of new observations and studies of cosmic opacity and cosmic dust at high redshifts for more realistic modelling of the evolution of the Universe.

Subject headings: early universe – cosmic background radiation – dust, extinction – universe opacity – dark energy

1. Introduction

Dust is an important component of the interstellar medium (ISM) and intergalactic medium (IGM), which interacts with the stellar radiation. Dust grains absorb and scatter the starlight and reemit the absorbed energy at infrared, far-infrared and microwave wavelengths (Mathis 1990; Schlegel et al. 1998; Calzetti et al. 2000; Draine 2003, 2011; Vavryčuk 2018). Since galaxies contain interstellar dust, they lose their transparency and become opaque. The most transparent galaxies are elliptical, while the spiral and irregular galaxies are more opaque, when more than 40% of light of stars in galaxies is absorbed by the galactic dust (Calzetti 2001; Holwerda et al. 2005, 2007; Finkelman et al. 2008; Lisenfeld et al. 2008). Similarly, the Universe is not transparent but partially opaque due to ambient cosmic dust. Absorption of light by intergalactic dust grains produces

cosmic opacity, which is spatially dependent and varies with frequency and redshift (Aguirre 1999a, 2000; Corasaniti 2006; Vavryčuk 2018, 2019). It can be measured by dust reddening being particularly appreciable at close distance from galaxies and in intracluster space (Chelouche et al. 2007; Muller et al. 2008; Ménard et al. 2010b). Ménard et al. (2010b) correlated the brightness of $\approx 85,000$ quasars at $z > 1$ with the position of 24×10^6 galaxies at $z \approx 0.3$ derived from the Sloan Digital Sky Survey, and found an averaged intergalactic attenuation A_V to about 0.03 mag.

Alternatively, the cosmic opacity can be estimated from the hydrogen column densities of Lyman α ($\text{Ly}\alpha$) absorbers. Massive clouds with $N_{\text{HI}} \approx 10^{21} \text{ cm}^{-2}$, called the damped $\text{Ly}\alpha$ absorbers (DLAs), are self-shielded and rich on cosmic dust. They are detected in galaxies as well as in the circumgalactic and in-

tergalactic space (Wolfe et al. 2005; Meiksin 2009; Ménard & Fukugita 2012; Peek et al. 2015; Tumlinson et al. 2017). Since a relation between the total hydrogen column density N_{H} and the color excess $E(B - V)$ is known: $N_{\text{H}}/E(B - V) = 5.6 - 5.8 \times 10^{21} \text{ cm}^{-2} \text{ mag}^{-1}$ (Bohlin et al. 1978; Rachford et al. 2002), we get the ratio $N_{\text{H}}/A_V \approx 1.87 \times 10^{21} \text{ cm}^{-2} \text{ mag}^{-1}$ for $R_V = 3.1$, which is a typical value for our Galaxy (Cardelli et al. 1989; Mathis 1990). From observations of the mean cross-section density of DLAs, $\langle n\sigma \rangle = (1.13 \pm 0.15) \times 10^{-5} h \text{ Mpc}^{-1}$ (Zwaan et al. 2005), the characteristic column density of DLAs, $N_{\text{HI}} \approx 10^{21} \text{ cm}^{-2}$, and the mean molecular hydrogen fraction in DLAs of about 0.4–0.6 (Rachford et al. 2002, their table 8), we obtain the cosmic opacity $\lambda_V \approx 1 - 2 \times 10^{-5} h \text{ Mpc}^{-1}$ at $z = 0$.

The cosmic opacity is very low in the local Universe (Chelouche et al. 2007; Muller et al. 2008), but it might steeply increase with redshift (Ménard et al. 2010b; Xie et al. 2015; Vavryčuk 2017b). Appreciable cosmic opacity at high redshift is documented by observations of (1) the evolution of the Ly α forest of absorption lines in quasar optical spectra, (2) the metallicity detected in the Ly α forest, and (3) emission spectra of high-redshift galaxies. In the Ly α forest studies, the evolution of massive Lyman-limit (LLS) and damped Lyman absorption (DLA) systems are, in particular, important, because they serve as reservoirs of dust (Wolfe et al. 2005; Meiksin 2009). It has been shown that the incidence rate and the Gunn-Peterson optical depth of the LLS and DLA systems increase with redshift as $(1+z)^4$ or more for $z < 7$ (Prochaska & Herbert-Fort 2004; Fan et al. 2006; Rao et al. 2006; Songaila & Cowie 2010), see Fig. 1. For higher z , the increase of the optical depth is even stronger.

Another independent indication of dust at high redshifts is a weak or no evolution of metallicity with redshift. For example, observations of the C_{IV} absorbers do not show any visible redshift evolution over cosmic time suggesting that a large fraction of intergalactic metals may already have been in place at $z > 6$ (Songaila 2001; Pettini et al. 2003; Ryan-Weber et al. 2006). In addition, the presence of dust in the high-redshift universe is documented by observations of dusty galaxies even at $z > 7$ (Watson et al. 2015; Laporte et al. 2017) and dusty halos around star-forming galax-

ies at $z = 5 - 7$ (Fujimoto et al. 2019). Zavala et al. (2015) measured a dust mass of $\approx 10^7 M_{\odot}$ for a galaxy at $z \approx 9$. Since dust in high-redshift galaxies can efficiently be transported to halos due to galactic wind (Aguirre 1999a,b) and radiation pressure (Hirashita & Inoue 2019), the cosmic dust must be present even at redshifts $z > 7 - 9$.

Since dust is traced mostly by reddening of galaxies and quasars at high redshifts, it is difficult to distinguish which portion of reddening is caused by dust present in a galaxy and by cosmic dust along the line of sight. Xie et al. (2015, 2016) studied dust extinction using spectra of $\approx 90,000$ quasars from the SDSS DR7 quasar catalogue and tried to separate both the effects. They revealed that quasars have systematically redder UV continuum slopes at higher redshifts and estimated the extinction A_V by cosmic dust of about $\approx 0.02 \text{ Gpc}^{-1}$. This value, however, strongly increases with redshift, because of increase of dust density due to the smaller volume of the Universe in the past (Vavryčuk 2017b; Vavryčuk 2018), see Fig. 2.

The fact that the Universe is not transparent but partially opaque might have fundamental cosmological consequences, because the commonly accepted cosmological model was developed for the transparent universe. Neglecting cosmic opacity produced by intergalactic dust may lead to distorting the observed evolution of the luminosity density and the global stellar mass density with redshift (Vavryčuk 2017b). For example, a decrease of the luminosity density with redshift observed for $z > 2 - 3$ is commonly explained by darkness of the early Universe. However, this effect can just be an artefact of non-negligible opacity of IGM in the early Universe, when the light coming from high redshifts is attenuated (Vavryčuk 2017b). Fig. 3 shows that after eliminating the effect of the opacity from observations, the comoving luminosity density and global stellar mass is redshift independent. Note that physical origin of darkness of the early Universe discussed here is quite different from that of 'dark ages' in the Big Bang theory. While we study the cosmic opacity due to the presence of dust at redshifts $z < 25$ (dust temperature being less than 80 K), the dark ages epoch is produced by opaque plasma at redshifts $z > 1100$ (plasma temperature being $\sim 10^9$ K).

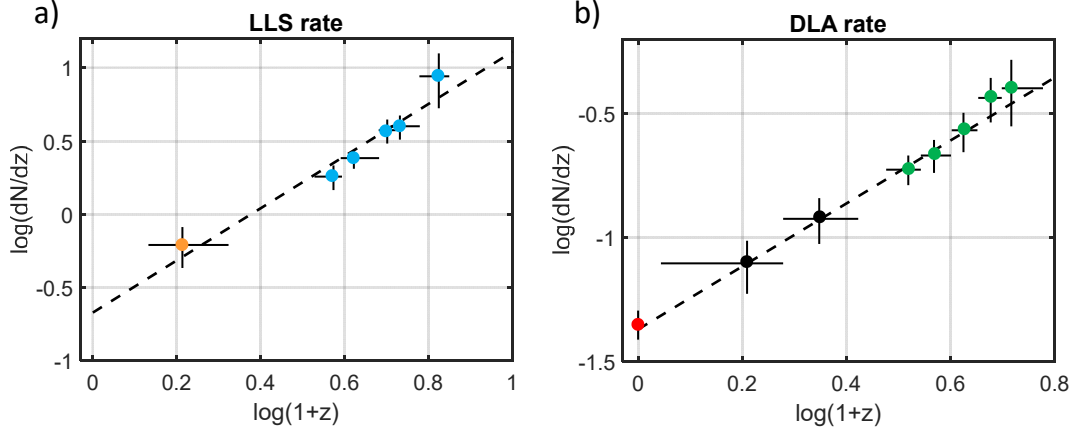


Fig. 1.— The incidence rate of the LLS (a) and DLA systems (b) as a function of redshift. The black dashed line - interpolation of observations. The observations are taken from Péroux et al. (2003) - orange dot, Songaila & Cowie (2010) - cyan dots, Zwaan et al. (2005) - red dot, Rao et al. (2006) - black dots, and Prochaska & Herbert-Fort (2004) - green dots.

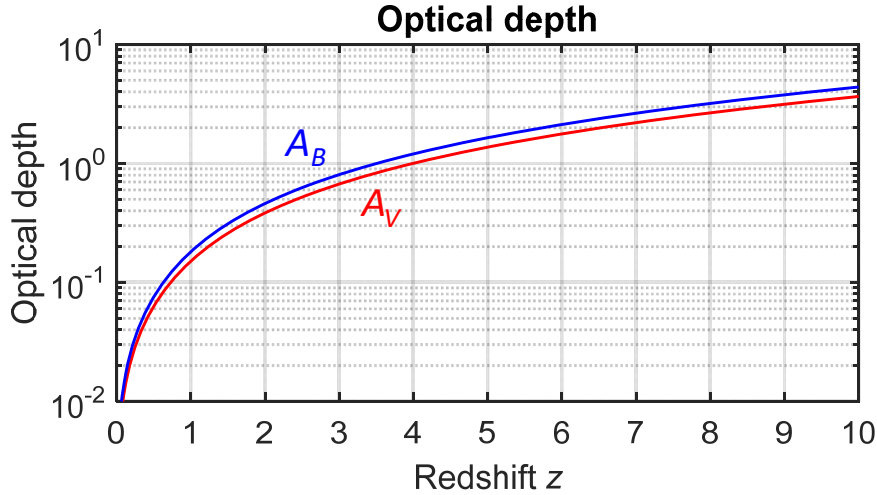


Fig. 2.— Optical depth of intergalactic space as a function of redshift. The extinction coefficient $R_V = A_V/(E(B - E))$ is assumed to be 5. A_V - extinction at the visual band, A_B - extinction at the B band. For details, see Vavryčuk (2017b); Vavryčuk (2018).

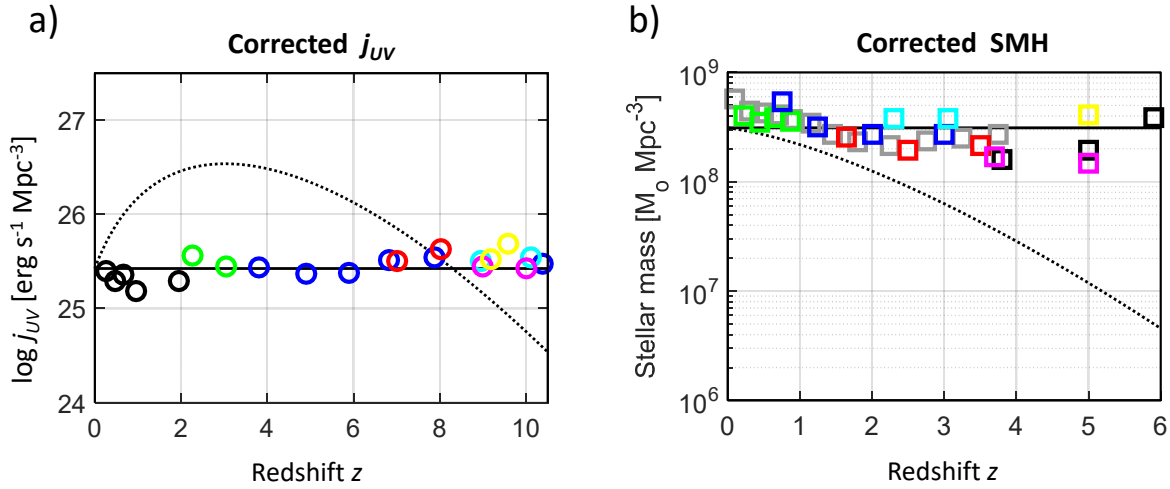


Fig. 3.— (a) The corrected comoving UV luminosity density j_{UV} as a function of redshift after eliminating the effect of the cosmic opacity defined by A_{UV} of $0.08 \text{ mag } h \text{ Gpc}^{-1}$. Observations are taken from Schiminovich et al. (2005, black circles), Reddy & Steidel (2009, green circles), Bouwens et al. (2014b, blue circles), McLure et al. (2013, red circles), Ellis et al. (2013, magenta circles), Oesch et al. (2014, cyan circles), and Bouwens et al. (2014a, yellow circles). The dotted line shows the apparent comoving luminosity density, when the bias produced by the cosmic opacity is not eliminated. (b) The comoving global stellar mass history (SMH) after eliminating the effect of the cosmic opacity defined by A_{UV} of $0.08 \text{ mag } h \text{ Gpc}^{-1}$. The colour squares show observations reported by Pérez-González et al. (2008, grey), Pozzetti et al. (2010, green), Kajisawa et al. (2009, blue), Marchesini et al. (2009, red), Reddy et al. (2012, cyan), González et al. (2011, black), Lee et al. (2012, magenta), and Yabe et al. (2009, yellow). The values are summarized in Table 2 of Madau & Dickinson (2014). The dotted line shows the apparent comoving SMH, when the bias produced by the cosmic opacity is not eliminated. For details, see Vavryčuk (2018).

Non-zero cosmic opacity may invalidate the interpretation of the Type Ia supernova (SNe Ia) dimming as a result of dark energy and the accelerating expansion of the Universe (Aguirre 1999a,b; Aguirre & Haiman 2000; Ménard et al. 2010a). According to Vavryčuk (2019) and Vavryčuk & Kroupa (2020), cosmic opacity $\lambda_B \approx 0.08 - 0.10 \text{ Gpc}^{-1}$ fits the Type Ia supernova observations with no need to introduce the accelerated expansion. In addition, cosmic dust can partly or fully produce the cosmic microwave background (CMB) (Wright 1982; Bond et al. 1991; Narlikar et al. 2003). For example, Vavryčuk (2018) showed that thermal radiation of dust is capable to explain the spectrum, intensity and temperature of the CMB including the CMB temperature/polarization anisotropies. In this theory, the CMB temperature fluctuations are caused by fluctuations of the extragalactic background light (EBL) produced by galaxy clusters and voids in the Universe, and the CMB polarization anomalies originate in the polarized thermal emission of needle-shaped conducting dust grains, which are aligned by magnetic fields around large-scale structures such as clusters and voids.

If cosmic opacity and light-matter interactions are considered, the Friedmann equations in the current form are inadequate and must be modified. The radiation pressure, which is caused by absorption of photons by dust grains and acts against gravitational forces, must be incorporated. In this paper, I demonstrate that the radiation pressure due to light absorption is negligible at the present epoch, but it could be significantly stronger in the past epochs. Surprisingly, its rise with redshift could be so steep that it could even balance the gravitational forces at high redshifts and cause the expansion of the Universe. Based on numerical modelling and observations of basic cosmological parameters, I show that the modified Friedmann equations avoid the initial singularity and lead to a cyclic model of the Universe with expansion/contraction epochs within a limited range of scale factors. I estimate the maximum redshift of the Universe achieved in the past and the maximum scale factor of the Universe in future.

2. Theory

2.1. Friedmann equations for the transparent universe

The standard Friedmann equations for the pressureless fluid read (Peacock 1999; Ryden 2016)

$$\left(\frac{\dot{a}}{a}\right)^2 = \frac{8\pi G}{3}\rho - \frac{kc^2}{a^2} + \frac{1}{3}\Lambda c^2, \quad (1)$$

$$\frac{\ddot{a}}{a} = -\frac{4\pi G}{3}\rho + \frac{1}{3}\Lambda c^2, \quad (2)$$

where $a = R/R_0 = (1+z)^{-1}$ is the relative scale factor, G is the gravitational constant, ρ is the mass density, k/a^2 is the spatial curvature of the universe, Λ is the cosmological constant, and c is the speed of light. Considering mass density ρ as a sum of matter and radiation contributions, we get

$$\frac{8\pi G}{3}\rho = H_0^2 [\Omega_m a^{-3} + \Omega_r a^{-4}]. \quad (3)$$

Eq. (1) is then rewritten as

$$H^2(a) = H_0^2 [\Omega_m a^{-3} + \Omega_r a^{-4} + \Omega_\Lambda + \Omega_k a^{-2}], \quad (4)$$

with the condition

$$\Omega_m + \Omega_r + \Omega_\Lambda + \Omega_k = 1, \quad (5)$$

where $H(a) = \dot{a}/a$ is the Hubble parameter, H_0 is the Hubble constant, and Ω_m , Ω_r , Ω_Λ and Ω_k are the normalized matter, radiation, vacuum and curvature terms. Assuming $\Omega_r = 0$ and $\Omega_k = 0$ in Eq. (4), we get the Λ CDM model

$$H^2(a) = H_0^2 [\Omega_m a^{-3} + \Omega_\Lambda], \quad (6)$$

which describes a flat, matter-dominated universe. The universe is transparent, because any interaction of radiation with matter is neglected. The vacuum term Ω_Λ is called dark energy and it is responsible for the accelerating expansion of the Universe. The dark energy is introduced into Eqs (4-6) to fit the Λ CDM model with observations of the Type Ia supernova dimming.

2.2. Light-matter interaction

The basic drawback of the Λ CDM model is its assumption of transparency of the Universe and the neglect of the universe opacity caused by interaction of light with intergalactic dust. Absorption

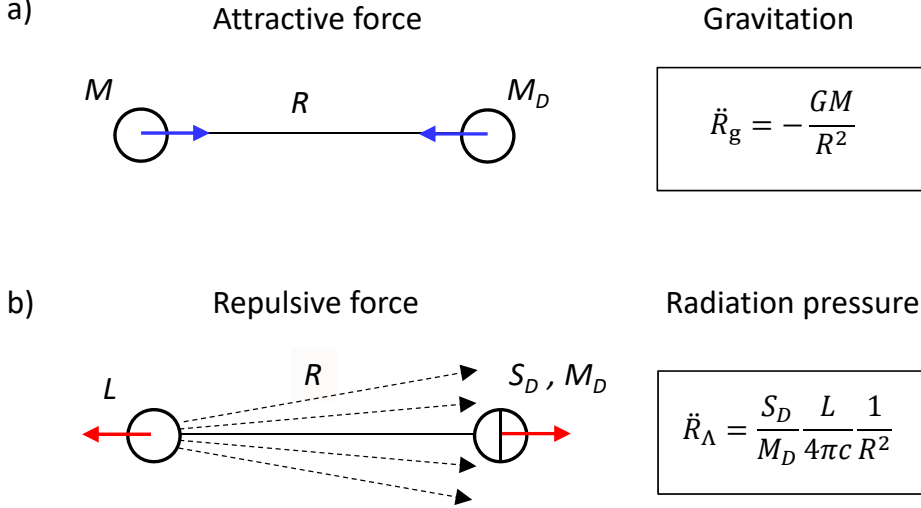


Fig. 4.— The scheme of gravitational forces (a) and radiation pressure (b) acting on dust grains. The blue and red arrows indicate a direction of the acting attractive and repulsive forces, respectively. The point source is characterized by mass M and luminosity L . The dust grains have mass M_D and the cross-section S_D . The radiation pressure caused by absorption of energy flux I emitted by the light source with luminosity L decreases with distance as $1/R^2$ similarly as the gravitational force.

of light by cosmic dust produces radiation pressure acting against the gravity, but this pressure is ignored in the Λ CDM model.

Let us consider light emitted by a point source with mass M and luminosity L (in W) and absorbed by a dust grain with mass M_D , see Fig. 4. The light source produces the energy flux I (in Wm^{-2}) and the radiation pressure p_D , which acts on the dust grain. The acceleration of the dust grain produced by the light source reads

$$\ddot{R}_\Lambda = \frac{S_D}{M_D} p_D, \quad (7)$$

where S_D is the absorption cross-section of the grain. Since the radiation pressure p_D is related to the energy flux I and to the luminosity L as

$$p_D = \frac{I}{c} = \frac{L}{4\pi R^2 c}, \quad (8)$$

we get

$$\ddot{R}_\Lambda = \frac{S_D}{M_D} \frac{L}{4\pi c} \frac{1}{R^2}, \quad (9)$$

where R is the distance of the dust grain from the light source, and c is the speed of light. The ratio

S_D/M_D in Eq. (9) can be expressed as

$$\frac{S_D}{M_D} = \frac{3}{4} \frac{Q_{\text{abs}}}{R_D \rho_D} = \kappa, \quad (10)$$

where $S_D = Q_{\text{abs}} \pi R_D^2$ is the absorption cross-section of the dust grain, $M_D = \frac{4}{3} \pi R_D^3 \rho_D$ is the mass of the grain, R_D is the grain radius, Q_{abs} is the grain absorption efficiency, ρ_D is the specific mass density of grains, and κ is the mass opacity (in $\text{m}^2 \text{kg}^{-1}$). Inserting Eq. (10) into Eq. (9), we write

$$\ddot{R}_\Lambda = \frac{\kappa L}{4\pi c} \frac{1}{R^2}. \quad (11)$$

Comparing the radiation-absorption acceleration \ddot{R}_Λ with the gravitational acceleration \ddot{R}_g

$$\ddot{R}_g = -\frac{GM}{R^2}, \quad (12)$$

we see that both accelerations depend on distance from a source in the same way (as $1/R^2$). Consequently, the total acceleration of a dust grain is

$$\ddot{R} = \ddot{R}_g + \ddot{R}_\Lambda = \frac{1}{R^2} \left(-GM + \frac{\kappa L}{4\pi c} \right). \quad (13)$$

Dividing Eq. (13) by distance R and substituting mass M (in kg) and luminosity L (in W) by mass density ρ (in kgm^{-3}) and luminosity density j (in Wm^{-3}), we get

$$\frac{\ddot{R}}{R} = -\frac{4\pi G}{3}\rho + \frac{\kappa j}{3c}, \quad (14)$$

and consequently, we obtain a generalized Poisson equation for the scalar potential Φ , which involves potentials for both gravitational and radiation-absorption fields

$$\Delta\Phi = 4\pi G\rho - \frac{\kappa j}{c}. \quad (15)$$

Equivalently

$$\Delta\Phi = 4\pi G\rho - \rho_\Lambda. \quad (16)$$

where $\rho_\Lambda = \kappa j/c$ will be called the density of the radiation-absorption field.

2.3. Friedmann equations for the opaque universe

The generalized Poisson equation (16) implies that the radiation-absorption term is in many aspects similar to gravity; its effect is, however, opposite. Therefore, deriving the Friedmann equations for the opaque universe using general relativity will be analogous to that for the transparent universe. The only difference is that we have to introduce another term into the Einstein field equations, which will describe a non-gravitational field associated with the light-matter interaction. This term will play the same role as the cosmological constant Λ in Eqs. (1-2), but in contrast to Λ , which is of unclear physical nature, the light-matter interaction term is physically well justified.

The light-matter interaction will be characterized by density ρ_Λ and pressure p_Λ . The energy-momentum tensor $\Lambda^{\mu\nu}$ of the light-matter interaction will be defined in a similar way as the energy-momentum tensor $T^{\mu\nu}$ for the gravitational field, see Appendix A for details. Assuming that the Universe is filled by a perfect homogeneous and isotropic fluid and its expansion is described by the standard FLRW metric, we obtain the following modified Friedmann equations (see Eqs. A11 and A15 in Appendix A):

$$\left(\frac{\dot{a}}{a}\right)^2 = \frac{8\pi G}{3}\rho - \frac{2}{3}\rho_\Lambda - \frac{kc^2}{a^2}, \quad (17)$$

$$\frac{\ddot{a}}{a} = -\frac{4\pi G}{3}(\alpha - 2)\rho + \frac{1}{3}(\beta - 2)\rho_\Lambda. \quad (18)$$

where coefficients α and β define the dependence of densities ρ and ρ_Λ on the scale factor $a(t)$: $\rho \sim a^{-\alpha}$ and $\rho_\Lambda \sim a^{-\beta}$. Specifying Eq. (18) for the pressureless fluid ($\alpha = 3$) and taking into account that $\rho_\Lambda = \kappa j/c$, we obtain the final form of the Friedmann equations for the opaque universe

$$\left(\frac{\dot{a}}{a}\right)^2 = \frac{8\pi G}{3}\rho - \frac{2}{3}\frac{\kappa j}{c} - \frac{kc^2}{a^2}, \quad (19)$$

$$\frac{\ddot{a}}{a} = -\frac{4\pi G}{3}\rho + \frac{\beta - 2}{3}\frac{\kappa j}{c}. \quad (20)$$

Comparing Eqs (1-2) with Eqs (19-20), we see that the modified Friedmann equations can be rewritten into a form almost identical with the original Friedmann equations

$$\left(\frac{\dot{a}}{a}\right)^2 = \frac{8\pi G}{3}\rho - \frac{kc^2}{a^2} + \frac{1}{3}\Lambda c^2, \quad (21)$$

$$\frac{\ddot{a}}{a} = -\frac{4\pi G}{3}\rho + \frac{2 - \beta}{2}\frac{1}{3}\Lambda c^2, \quad (22)$$

if the cosmological term Λ is defined as

$$\Lambda = 2\frac{\kappa j}{c^3}. \quad (23)$$

The only difference is in factor $(2 - \beta)/2$ in Eq. (22), originating from the fact that Λ is not a constant any more but it depends on the scale factor $a(t)$. If $\beta = 0$, Eq. (22) becomes identical with the Friedmann equation (2).

2.4. Distance-redshift relation

Assuming that Λ depends on a as $\sim a^{-\beta}$ in Eq. (21), the Hubble parameter reads

$$H^2(a) = H_0^2 [\Omega_m a^{-3} + \Omega_r a^{-4} + \Omega_a a^{-\beta} + \Omega_k a^{-2}], \quad (24)$$

where Ω_m , Ω_r , Ω_a and Ω_k are the normalized matter, radiation, radiation-absorption and curvature terms, respectively. In contrast to Ω_m and Ω_r , which describe attractive gravitational forces produced by matter and radiation in the Universe, Ω_a describes repulsive non-gravitational forces produced by the light-matter interaction. Since gravity associated with radiation is non-negligible only for $z > 1100$, we can assume $\Omega_r = 0$ and specify

Eq. (24) for the matter-dominated opaque universe as

$$H^2(a) = H_0^2 [\Omega_m a^{-3} + \Omega_a a^{-\beta} + \Omega_k a^{-2}] , \quad (25)$$

with the condition

$$\Omega_m + \Omega_a + \Omega_k = 1 , \quad (26)$$

where

$$\Omega_m = \frac{1}{H_0^2} \left(\frac{8\pi G}{3} \rho_0 \right) , \quad (27)$$

$$\Omega_a = -\frac{1}{H_0^2} \left(\frac{2}{3} \frac{\kappa_0 j_0}{c} \right) , \quad (28)$$

$$\Omega_k = -\frac{kc^2}{H_0^2} . \quad (29)$$

The minus sign in Eq. (28) means that the radiation pressure due to the light-matter interaction acts against the gravity. Considering $a = 1/(1+z)$, the comoving distance is expressed from Eq. (25) as a function of redshift as follows

$$dr = \frac{c}{H_0} \frac{dz}{\sqrt{\Omega_m (1+z)^3 + \Omega_a (1+z)^\beta + \Omega_k (1+z)^2}} . \quad (30)$$

2.5. Redshift dependence of the light-matter interaction

The radiation-absorption term Λ defined in Eq. (23) is redshift dependent. Under the assumption that the number of sources and their luminosity conserves in time, the rest-frame luminosity density j_ν for a given frequency ν depends on redshift as $(1+z)^3$ and the bolometric luminosity density j depends on redshift as

$$j = j_0 a^{-4} = j_0 (1+z)^4 . \quad (31)$$

where subscript '0' corresponds to the quantity observed at present. The assumption of the independence of the global stellar mass in the Universe looks apparently unrealistic but it is fully consistent with observations if corrections to opacity of the high-redshift Universe are applied (Vavryčuk 2017b; Vavryčuk 2018), see Fig. 3.

The luminosity density comprises energy radiated by galaxies into the intergalactic space and thermal radiation of intergalactic dust. All these sources produce cosmic background radiation in

the Universe being the sum of the cosmic X-ray background (CXB), the extragalactic background light (EBL) and the cosmic microwave background (CMB). The cosmic background radiation as any radiation in the expanded universe depends on redshift as

$$I = I_0 a^{-4} = I_0 (1+z)^4 . \quad (32)$$

Also the mass opacity κ in Eq. (23) depends on redshift. Based on the extinction law, the mass opacity κ depends on the wavelength λ of absorbed radiation as $\lambda^{-\gamma}$, where γ is the spectral index ranging between 1.0 and 2.0 for grains with size of 0.2 μm or smaller (Mathis et al. 1977; Draine 2011), see Fig. 5. Hence, if radiation changes its wavelength due to the redshift, the opacity κ is also redshift dependent. Consequently, the coefficient β describing the redshift-dependent radiation-absorption term in Eqs (25) and (30) ranges from 5 to 6. By contrast, the mass opacity is wavelength independent for large grains with size larger than wavelength λ and the radiation-absorption term depends on z as $(1+z)^4$ only.

Since the coefficient β essentially affects behaviour of the Hubble parameter $H(a)$ and subsequently the evolution of the Universe, we will discuss the origins of its enormously high value in details. The normalized matter and radiation terms Ω_m and Ω_r in Eq. (24) depend on the scale factor a as a^{-3} and a^{-4} , respectively. Hence, one would intuitively expect that the interaction of matter with radiation will produce term $a^{-\beta}$ with β ranging between 3 and 4. However, this speculation is false, because it ignores essential property of the radiation-matter interaction - its frequency dependence. The interaction of radiation with matter is caused by absorption of light by grains of cosmic dust, which depends on the wavelength of light and on the size of dust grains. While large wavelengths of light are absorbed weakly, the short wavelengths are absorbed more intensely. Hence, three effects are involved in the light-matter interaction: (1) an increase of the intensity of light as $(1+z)^3$ associated with decreasing the volume of the Universe with redshift, (2) an additional increase of the intensity of light as $(1+z)$ due to the shortening of wavelengths of photons caused by the cosmological redshift, and (3) an increase of light absorption as $(1+z)^\gamma$, with γ ranging be-

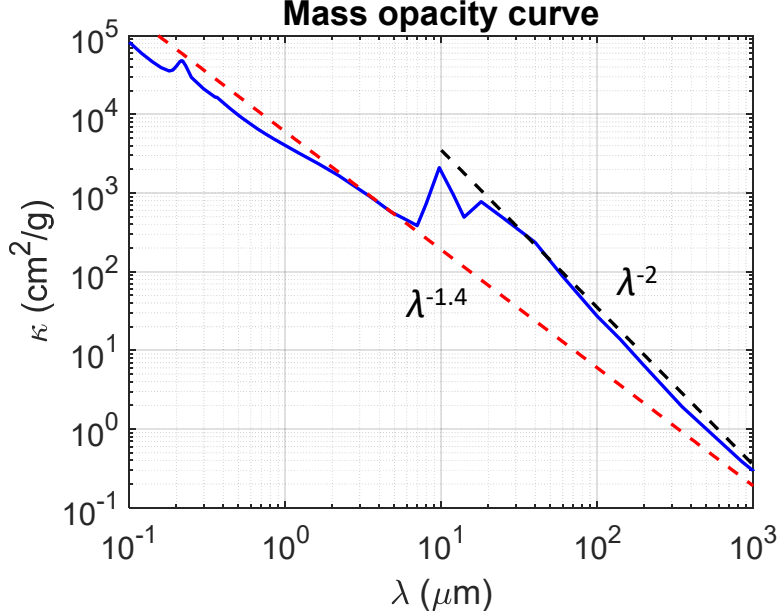


Fig. 5.— The mass opacity κ as a function of wavelength for the so-called MRN dust model (Mathis et al. 1977) defined by the power-law grains-size distribution with lower and upper size limits between ~ 5 and ~ 250 nm, see Tables 4-6 of Draine (2003). The black and red dashed lines show the long-wavelength asymptotic behaviour predicted by the power law with the spectral index of 2 and 1.4, respectively.

tween 1 and 2, because the photons at high redshifts have shorter wavelengths and interact much strongly with cosmic dust grains than photons at the present epoch.

2.6. Limits of the scale factor a

In order to get simple closed-form formulas, we assume in the next that the mean spectral index γ characterizing the absorption of light by mixture of grains of varying size is 1. Consequently, the radiation-absorption term depends on a as $\sim a^{-5}$. The scale factor a of the Universe with the zero expansion rate is defined by the zero Hubble parameter in Eq. (25), which yields a cubic equation in a

$$\Omega_k a^3 + \Omega_m a^2 + \Omega_a = 0. \quad (33)$$

Taking into account that $\Omega_m > 0$ and $\Omega_a < 0$, Eq. (33) has two distinct real positive roots for

$$\left(\frac{\Omega_m}{3}\right)^2 > \left(\frac{\Omega_k}{2}\right)^2 |\Omega_a| \quad \text{and} \quad \Omega_k < 0. \quad (34)$$

Negative Ω_a and Ω_k imply that

$$\Omega_m > 1 \quad \text{and} \quad \rho_0 > \rho_c = \frac{8\pi G}{3H_0^2}. \quad (35)$$

Under these conditions, Eq. (25) describes a universe with a cyclic expansion/contraction history and the two real positive roots a_{\min} and a_{\max} define the minimum and maximum scale factors of the Universe. For $\Omega_a \ll 1$, the scale factors a_{\min} and a_{\max} read approximately

$$a_{\min} \cong \sqrt{\left|\frac{\Omega_a}{\Omega_m}\right|} \quad \text{and} \quad a_{\max} \cong \left|\frac{\Omega_m}{\Omega_k}\right|, \quad (36)$$

and the maximum redshift is

$$z_{\max} = \frac{1}{a_{\min}} - 1. \quad (37)$$

The scale factors a of the Universe with the maximum expansion/contraction rates are defined by

$$\frac{d}{da} H^2(a) = 0, \quad (38)$$

which yields a cubic equation in a

$$2\Omega_k a^3 + 3\Omega_m a^2 + 5\Omega_a = 0. \quad (39)$$

Taking into account Eqs (21-22) and Eqs (27-29), the deceleration of the expansion reads

$$\ddot{a} = -\frac{1}{2}H_0^2 [\Omega_m a^{-2} + 3\Omega_a a^{-4}] . \quad (40)$$

Hence, the zero deceleration is for the scale factor

$$a = \sqrt{\left| \frac{3\Omega_a}{\Omega_m} \right|} . \quad (41)$$

The above equations are quite simple, because they are derived for the spectral index $\gamma = 1$. For other values of γ , the limits of the scale factor a are obtained by solving the equation for the zero Hubble parameter numerically. In general, the higher spectral index γ , the smaller value of the maximum redshift z_{\max} , see the next sections.

3. Parameters for modelling

For calculating the expansion history and cosmic dynamics of the Universe, we need observations of the mass opacity of intergalactic dust grains, the galaxy luminosity density, the mean mass density, and the expansion rate and curvature of the Universe at the present time.

3.1. Mass opacity of cosmic dust

When estimating the mass opacity of dust, κ_0 , we have to know basic parameters of dust grains. The size d of dust grains is in the range of $0.01 - 0.2 \mu\text{m}$ with a power-law distribution d^{-q} with $q = 3.5$ (Mathis et al. 1977; Jones et al. 1996), but silicate and carbonaceous grains dominating the scattering are typically with $d \approx 0.1 \mu\text{m}$ (Draine & Fraisse 2009; Draine 2011). The grains of size $0.07 \mu\text{m} \leq d \leq 0.2 \mu\text{m}$ are also ejected to the IGM most effectively (Davies et al. 1998; Bianchi & Ferrara 2005). The grains form complicate fluffy aggregates, which are often elongated or needle-shaped (Wright 1982, 1987). Considering the density of carbonaceous material $\rho \approx 2.2 \text{ g cm}^{-3}$ and the silicate density $\rho \approx 3.8 \text{ g cm}^{-3}$ (Draine 2011), the average density of porous dust grains is $\approx 2 \text{ g cm}^{-3}$ or less (Flynn 1994; Kocifaj et al. 1999; Kohout et al. 2014). Consequently, the standard dust models (Weingartner & Draine 2001) predict the wavelength-dependent mass opacity. For example, Draine (2003) reports the mass opacity of $855 \text{ m}^2 \text{ kg}^{-1}$ at the V-band and

the mass opacity of $402 \text{ m}^2 \text{ kg}^{-1}$ for a wavelength of $1 \mu\text{m}$, which corresponds to the maximum intensity of the EBL.

3.2. EBL and the galaxy luminosity density

The EBL covers a wide range of wavelengths from 0.1 to $1000 \mu\text{m}$. It was measured, for example, by the IRAS, FIRAS, DIRBE on COBE, and SCUBA instruments; for reviews, see Hauser & Dwek (2001); Lagache et al. (2005); Cooray (2016). The direct measurements are supplemented by integrating light from extragalactic source counts (Madau & Pozzetti 2000; Hauser & Dwek 2001) and by attenuation of gamma rays from distant blazars due to scattering on the EBL (Kneiske et al. 2004; Dwek & Krennrich 2005; Primack et al. 2011; Gilmore et al. 2012). The EBL spectrum has two maxima: associated with the radiation of stars (at $0.7 - 2 \mu\text{m}$) and with the thermal radiation of dust in galaxies (at $100 - 200 \mu\text{m}$), see Schlegel et al. (1998); Calzetti et al. (2000). Despite extensive measurements, uncertainties of the EBL are still large. The total EBL should fall between 40 and $200 \text{ nW m}^{-2} \text{ sr}^{-1}$ (Vavryčuk 2018, his fig. 1) with the most likely value $I^{\text{EBL}} = 80 - 100 \text{ nW m}^{-2} \text{ sr}^{-1}$ (Hauser & Dwek 2001; Bernstein et al. 2002a,b,c; Bernstein 2007).

The galaxy luminosity density is determined from the Schechter function (Schechter 1976). It has been measured by large surveys 2dFGRS (Cross et al. 2001), SDSS (Blanton et al. 2001, 2003) or CS (Brown et al. 2001). The luminosity function in the R-band was estimated at $z = 0$ to be $(1.84 \pm 0.04) \times 10^8 h L_\odot \text{ Mpc}^{-3}$ for the SDSS data (Blanton et al. 2003) and $(1.9 \pm 0.6) \times 10^8 h L_\odot \text{ Mpc}^{-3}$ for the CS data (Brown et al. 2001). The bolometric luminosity density is estimated by considering the spectral energy distribution (SED) of galaxies averaged over different galaxy types, being thus about 1.7 times larger than that in the R-band (Vavryčuk 2017b, his table 2): $j_0 \approx 3.1 \times 10^8 h L_\odot \text{ Mpc}^{-3}$.

3.3. Matter density of the Universe

A simplest and most straightforward method, how to estimate the matter density, is based on galaxy surveys and computation of the mass from

the observed galaxy luminosity and from the mass-to-light ratio (M/L) that reflects the total amount of the mass relative to the light within a given scale. The M/L ratio is, however, scale dependent and increases from bright, luminous parts of galaxies to their halos (with radius of ≈ 200 kpc) formed by (baryonic and/or speculative non-baryonic) dark matter. The M/L ratio depends also on a galaxy type being about 3 to 4 times larger for elliptical/SO galaxies than for typical spirals, hence the observed M/L_B is $\approx 100h$ for spirals, but $\approx 400h$ for ellipticals at radius of ≈ 200 kpc, see Bahcall et al. (1995). Considering the mean asymptotic ratio M/L_B of $200 - 300h$ and the observed mean luminosity density of the Universe at $z = 0$ of $\approx 2.5 \times 10^8 h L_\odot \text{Mpc}^{-3}$ reported by Cross et al. (2001), the matter density Ω_m associated with galaxies is about $0.2 - 0.3$ ($\Omega_m = 1$ means the critical density).

Another source of matter in the universe is connected to Ly α absorbers containing photoionized hydrogen at $\approx 10^4$ K and being detected by the Ly α forest in quasar spectra (Meiksin 2009). These systems are partly located in the galaxy halos, but a significant portion of them cannot be associated to any galaxy, being observed, for example, in voids (Penton et al. 2002; Tejos et al. 2012, 2014). The Ly α absorbers also form the intragroup and intracluster medium (Bielby et al. 2017) and the intergalactic medium nearby the other large-scale galaxy structures like the galaxy filaments (Tejos et al. 2014; Wakker et al. 2015). In addition, it is speculated that large amount of matter is located in the warm-hot intergalactic medium (WHIM) that is a gaseous phase of moderate to low density ($\approx 10 - 30$ times the mean density of the Universe) and at temperatures of $10^5 - 10^7$ K. Although it is difficult to observe the WHIM because of low column densities of HI in the hot gas, they might be potentially detected by surveys of broad HI Ly α absorbers (BLAs) as reported by Nicastro et al. (2018) or Pessa et al. (2018).

Hence, we conclude that the estimate of matter density $\Omega_m = 0.2 - 0.3$ inferred from a distribution of galaxies is just a lower limit, while the upper limit of Ω_m is unconstrained being possibly close to or even higher than 1. This statement contradicts the commonly accepted value of $\Omega_m = 0.3$ reported by Planck Collaboration et al. (2016a,

2018) which is based on the interpretation of the CMB as a relic radiation of the Big Bang.

3.4. Hubble constant and cosmic curvature

The Hubble constant H_0 is measured by methods based on the Sunyaev-Zel'dovich effect (Birkinshaw 1999; Carlstrom et al. 2002; Bonamente et al. 2006) or gravitational lensing (Suyu et al. 2013; Bonvin et al. 2017), gravitational waves (Abbott et al. 2017; Vitale & Chen 2018; Howlett & Davis 2020) or acoustic peaks in the CMB spectrum provided by Planck Collaboration et al. (2016a), and they yield values mostly ranging between 67 and $74 \text{ km s}^{-1} \text{Mpc}^{-1}$. Among these approaches, direct methods are considered to be most reliable and accurate (for a review, see Jackson (2015)). These methods are based on measuring local distances up to $20 - 30$ Mpc using Cepheid variables observed by the Hubble Space Telescope (HST). The HST galaxies with distance measured with the Cepheid variables are then used to calibrate the SNe Ia data. With this calibration, the distance measure can be extended to other more distant galaxies (hundreds of Mpc) in which SNe Ia are detected (Freedman et al. 2001; Riess et al. 2011). The estimate of H_0 obtained by Riess et al. (2016) using the Cepheid calibration is $73.25 \pm 1.74 \text{ km s}^{-1} \text{Mpc}^{-1}$. The precision of the distance scale was further reduced by a factor of 2.5 by Riess et al. (2018). Another estimate of H_0 obtained by Freedman et al. (2019) using the SNe Ia with a red giant branch calibration is $69.8 \pm 2.5 \text{ km s}^{-1} \text{Mpc}^{-1}$.

Assuming the Λ CDM model, the CMB and BAO observations indicate a nearly flat Universe (Planck Collaboration et al. 2016a). This method is not, however, model independent and ignores an impact of cosmic dust on the CMB. A model-independent method proposed by Clarkson et al. (2007) is based on reconstructing the comoving distances by Hubble parameter data and comparing with the luminosity distances (Li et al. 2016; Wei & Wu 2017) or the angular diameter distances (Yu & Wang 2016). The cosmic curvature can also be constrained using strongly gravitational lensed SNe Ia (Qi et al. 2019) and using lensing time delays and gravitational waves (Liao 2019). The authors report the curvature term Ω_k ranging between -0.3 to 0 indicating a closed universe, not

significantly departing from flat geometry.

4. Results

Estimating the required cosmological parameters from observations, the upper and lower limits of the volume of the Universe and the evolution of the Hubble parameter with time can be calculated using Eqs (25-29). The mass density of the Universe higher than the critical density is considered, and subsequently Ω_m is higher than 1. The Hubble constant is $H_0 = 69.8 \text{ km s}^{-1} \text{ Mpc}^{-1}$, taken from Freedman et al. (2019). The mass opacity κ_0 of $402 \text{ m}^2 \text{ kg}^{-1}$ is taken from table 4 of Draine (2003) and it characterizes the opacity of dust at a wavelength of $1 \text{ } \mu\text{m}$. The opacity is further multiplied by factor ε reflecting that dust grains are not spherical but rather prolate spheroids having a larger effective cross-section. The luminosity density is $j_0 = 3.1 \times 10^8 \text{ h } L_\odot \text{ Mpc}^{-3}$. The radiation-absorption term in Eq. (28) is multiplied by a factor of 2, because photons are not only absorbed but also radiated by dust grains to maintain the thermal equilibrium. The exponent β of the power-law decay of the radiation-absorption term in Eq. (25) ranges from 5.2 to 5.6. The results of modelling are summarized in Table 1.

As seen in Fig. 6, the maximum redshift of the Universe depends on Ω_m and Ω_a , and ranges from 13 to 18 for $\beta = 5.4$. In contrast to a_{\min} depending on both Ω_m and Ω_a , the maximum scale factor a_{\max} of the Universe depends primarily on Ω_m only. Fig. 7 shows that a_{\max} rapidly decreases with increasing Ω_m . Obviously, the limiting value is $\Omega_m = 1$, when a_{\max} is infinite. The limiting value is $\Omega_m = 1$, when a_{\max} is infinite. For $\Omega_m = 1.1, 1.2, 1.3$ and 1.5 , the scale factor a_{\max} is 11.2, 6.0, 4.4 and 3.0, respectively.

The history of the Hubble parameter $H(z)$ and its evolution in the future $H(a)$ calculated by Eq. (25) is shown in Fig. 8 for five scenarios summarized in Table 1. The form of $H(z)$ in Fig. 8a is controlled by Ω_a and the power-law exponent β , while the form of $H(a)$ in Fig. 8b is controlled by Ω_m . The Hubble parameter $H(z)$ increases with redshift up to its maximum. After that the function rapidly decreases to zero. The drop of $H(z)$ is due to a fast increase of light attenuation producing strong repulsive forces at high redshift. For future epochs, function $H(a)$ is pre-

dicted to monotonously decrease to zero. The rate of decrease is controlled just by gravitational forces; the repulsive forces originating in light attenuation are negligible. For a comparison, Fig. 8 (red line) shows the Hubble parameter $H(a)$ for the standard Λ CDM model (Planck Collaboration et al. 2016a), which is described by Eq. (6) with $\Omega_m = 0.3$ and $\Omega_\Lambda = 0.7$.

The distance-redshift relation of the proposed cyclic model of the Universe is quite different from the standard Λ CDM model (see Fig. 9). In both models, the comoving distance monotonously increases with redshift, but the redshift can go possibly to 1000 or more in the standard model, while the maximum redshift is likely 14-15 in the optimum cyclic model. The increase of distance with redshift is remarkably steeper for the Λ CDM model than for the cyclic model. The ratio between distances in the cyclic and Λ CDM models rapidly decreases from 1 at $z = 0$ to about 0.63 at $z > 4$.

5. Other supporting evidence

The cyclic cosmological model of the opaque universe successfully removes some tensions of the standard Λ CDM model:

- The model does not limit the age of stars in the Universe. For example, observations of a nearby star HD 140283 (Bond et al. 2013) with age of $14.46 \pm 0.31 \text{ Gyr}$ are in conflict with the age of the Universe, $13.80 \pm 0.02 \text{ Gyr}$, determined from the interpretation of the CMB as relic radiation of the Big Bang (Planck Collaboration et al. 2016a).
- The model predicts the existence of very old mature galaxies at high redshifts. The existence of mature galaxies in the early Universe was confirmed, for example, by Watson et al. (2015) who analyzed observations of the Atacama Large Millimetre Array (ALMA) and revealed a galaxy at $z > 7$ highly evolved with a large stellar mass and heavily enriched in dust. Similarly, Laporte et al. (2017) analyzed a galaxy at $z \approx 8$ with a stellar mass of $\approx 2 \times 10^9 M_\odot$ and a dust mass of $\approx 6 \times 10^6 M_\odot$. Large amount of dust is reported by Venemans et al. (2017) for a quasar at $z = 7.5$ in the interstellar medium

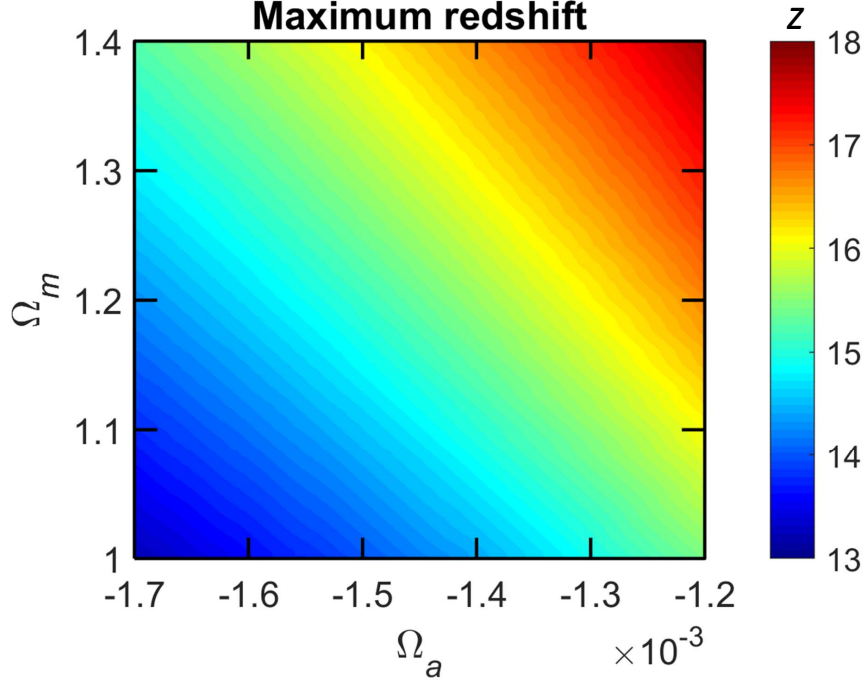


Fig. 6.— Maximum redshift as a function of Ω_m and Ω_a . The power-law exponent β describing a decay of the radiation-absorption term with the scale factor a is assumed to be 5.4, see Table 1.

Table 1: Maximum redshift and scale factor in the cyclic model of the opaque universe

Model	Input parameters					Output	
	ε	Ω_m	Ω_a	β	Ω_k	a_{\max}	z_{\max}
A	6	1.2	-1.7×10^{-3}	5.6	-0.198	6.1	11.4
B	4	1.2	-1.2×10^{-3}	5.2	-0.199	6.0	22.0
C	5	1.2	-1.5×10^{-3}	5.4	-0.199	6.0	15.1
D	5	1.1	-1.5×10^{-3}	5.4	-0.099	11.2	14.6
E	5	1.3	-1.5×10^{-3}	5.4	-0.299	4.4	15.6

Parameter ε is the ratio of the spheroidal to spherical dust grain cross-sections, Ω_m , Ω_a , and Ω_k are the matter, radiation-absorption and curvature terms, β is the power-law exponent describing a decay of the radiation-absorption term with the scale factor a in Eq. (25), and a_{\max} and z_{\max} are the estimates of the maximum scale factor and redshift, respectively. Models A, B and C predict low, high and optimum values of z_{\max} . Models E, D and C predict low, high and optimum values of a_{\max} .

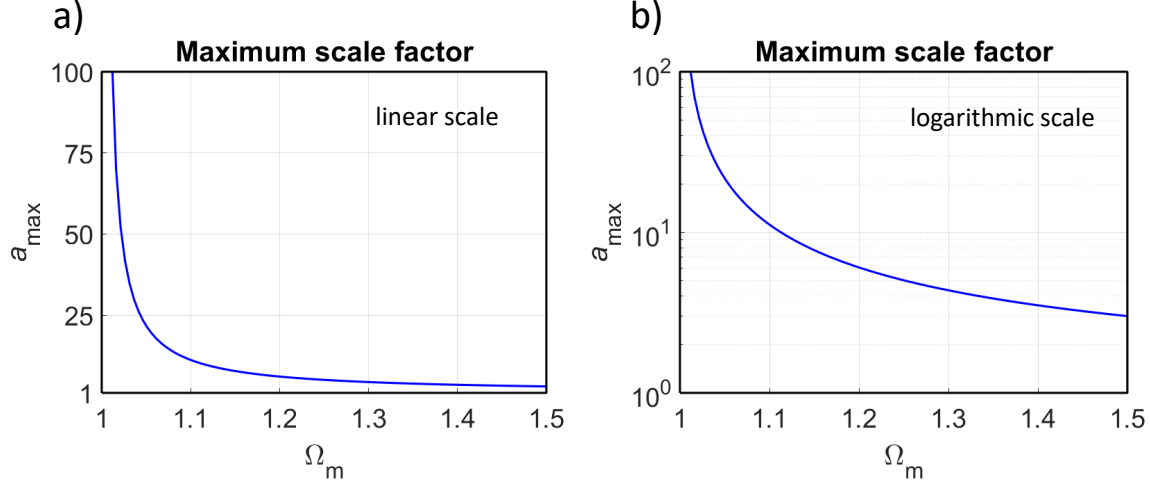


Fig. 7.— The maximum scale factor as a function of Ω_m . (a) Linear scale, (b) logarithmic scale. The dependence on Ω_a is negligible.

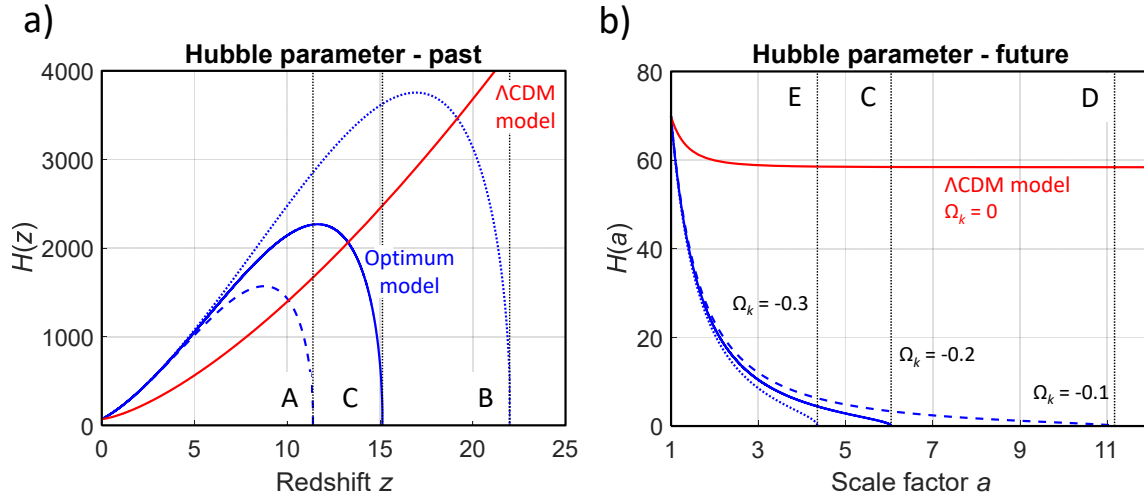


Fig. 8.— The evolution of the Hubble parameter with redshift in the past and with the scale factor in the future (in $\text{km s}^{-1} \text{Mpc}^{-1}$). (a) The blue dashed, dotted and solid lines show Models A, B and C in Table 1. (b) The blue solid, dashed, and dotted lines show Models C, D and E in Table 1. The black dotted lines mark the predicted maximum redshifts (a) and maximum scale factors (b) for the models considered. The red solid line shows the flat Λ CDM model with $H_0 = 69.8 \text{ km s}^{-1} \text{Mpc}^{-1}$, taken from Freedman et al. (2019), and with $\Omega_m = 0.3$ and $\Omega_\Lambda = 0.7$.

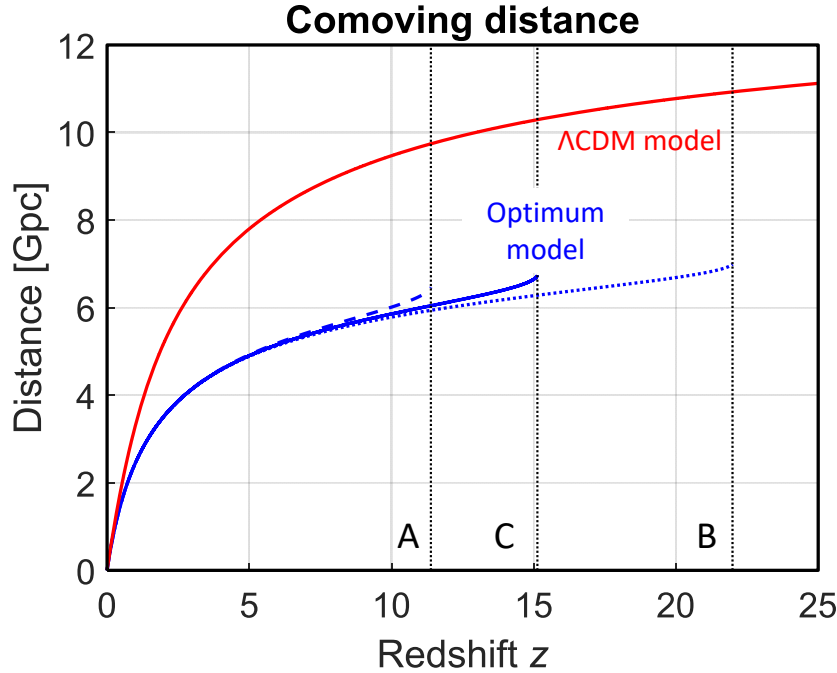


Fig. 9.— Comoving distance as a function of redshift z . The blue dashed, dotted and solid lines show Models A, B and C in Table 1. The black dotted lines mark the predicted maximum redshifts for the models considered. The red solid line shows the flat Λ CDM model with $H_0 = 69.8 \text{ km s}^{-1} \text{ Mpc}^{-1}$, taken from Freedman et al. (2019), and with $\Omega_m = 0.3$ and $\Omega_\Lambda = 0.7$.

of its host galaxy. In addition, a remarkably bright galaxy at $z \approx 11$ was found by Oesch et al. (2016) and a significant increase in the number of galaxies for $8.5 < z < 12$ was reported by Ellis et al. (2013). Note that the number of papers reporting discoveries of galaxies at $z \approx 10$ or higher is growing rapidly (Hashimoto et al. 2018; Hoag et al. 2018; Oesch et al. 2018; Salmon et al. 2018).

- The model is capable to explain the SNe Ia dimming discovered by Riess et al. (1998) and Perlmutter et al. (1999) without introducing dark energy as the hypothetical energy of vacuum (Vavryčuk 2019), which is difficult to explain under quantum field theory (Weinberg et al. 2013). Moreover, the speed of gravitational waves and the speed of light differ for most of dark energy models (Sakstein & Jain 2017; Ezquiaga & Zumalacárregui 2017), but observations of the binary neutron star merger GW170817 and its electromagnetic counterparts proved that both speeds coincide with a high accuracy.

- The model avoids a puzzle, how the CMB as relic radiation could survive the whole history of the Universe without any distortion (Vavryčuk 2017a) and why several unexpected features at large angular scales such as non-Gaussianity (Vielva et al. 2004; Cruz et al. 2005; Planck Collaboration et al. 2014) and a violation of statistical isotropy and scale invariance are observed in the CMB.
- The temperature of the CMB as thermal radiation of cosmic dust is predicted with the accuracy of 2%, see Vavryčuk (2018). The CMB temperature is controlled by the EBL intensity and by the ratio of galactic and intergalactic opacities. The temperature of intergalactic dust increases linearly with redshift and exactly compensates the change of wavelengths due to redshift. Consequently, dust radiation looks apparently like the blackbody radiation with a single temperature.
- The model explains satisfactorily: (1) the observed bolometric intensity of the EBL with a value of $\approx 100 \text{ nW m}^{-1} \text{ sr}^{-1}$, see

Vavryčuk (2017b), (2) the redshift evolution of the comoving UV luminosity density with extremely high values at redshifts $2 < z < 4$, see Vavryčuk (2018) (his fig. 11), and (3) a strong decay of the global stellar mass density at high redshifts, see Vavryčuk (2018) (his fig. 12). The increase of the luminosity density at $z \approx 2 - 3$ does not originate in the evolution of the star formation rate as commonly assumed but in the change of the proper volume of the Universe. The decrease of the luminosity density at high z originates in the opacity of the high-redshift universe.

Note that the prediction of a close connection between the CMB anisotropies and the large-scale structures is common to both the standard model and the opaque universe model. The arguments are, however, reversed. The Big Bang theory assumes that the large-scale structures are a consequence of the CMB fluctuations originated at redshifts $z \approx 1100$, while the opaque universe model considers the CMB fluctuations as a consequence of the large-scale structures at redshifts less than $3 - 5$. The polarization anomalies of the CMB correlated with temperature anisotropies are caused by the polarized thermal emission of needle-shaped conducting dust grains aligned by large-scale magnetic fields around clusters and voids. The phenomenon is analogous to the polarized interstellar dust emission in our Galaxy, which is observed at shorter wavelengths because the temperature of the galactic dust is higher than that of the intergalactic dust (Lazarian & Prunet 2002; Gold et al. 2011; Ichiki 2014; Planck Collaboration et al. 2015, 2016b).

6. Discussion

The standard Friedmann equations were derived for the transparent universe and assume no light-matter interaction. The equations contain densities Ω_m and Ω_r that describe the effects of gravity produced by matter, radiation and radiation pressure of photon gas. Since radiation pressure represents energy, it produces also gravity according to general relativity. The effects of radiation are, however, significant only for $z > 1100$. The modified Friedmann equations contain another density Ω_a , which is also connected with the radiation pressure but in a different way. This

pressure is produced by absorption of photons by ambient cosmic dust and it acts against gravity.

The radiation pressure as a cosmological force acting against the gravity has not been proposed yet, even though its role is well known in the stellar dynamics (Kippenhahn et al. 2012). The radiation pressure is important in the evolution of massive stars (Zinnecker & Yorke 2007), in supernovae stellar winds and in galactic wind dynamics (Aguirre 1999b; Martin 2005; Hopkins et al. 2012; Hirashita & Inoue 2019). Apparently, the radiation pressure in the evolution of the Universe was overlooked, because the Universe was assumed to be transparent. By contrast, the role of radiation pressure is essential in the opaque universe model, because it is produced by absorption of photons by cosmic dust. Since the cosmic opacity and the intensity of the EBL steeply rise with redshift (see Fig. 2), the radiation pressure, negligible at present, becomes significant at high redshifts and can fully eliminate gravity and stop the universe contraction. In this process, small dust grains will probably be more important, because the mass opacity responsible for the radiation pressure rapidly increases with decreasing size of grains. Similarly, the emission of high-energy photons will affect the universe dynamics more distinctly than the photons re-emitted by dust grains which form the CMB. The high-energy photons emitted by stars are absorbed by 3-4 orders more efficiently compared to the CMB photons, which are absorbed by dust very weakly.

Hence, the expansion/contraction evolution of the Universe might be a result of imbalance of gravitational forces and radiation pressure. Since the comoving global stellar and dust masses are basically independent of time with minor fluctuations only (see Fig. 3), the evolution of the Universe is stationary. The age of the Universe in the cyclic model is unconstrained and galaxies can be observed at any redshift less than the maximum redshift z_{\max} . The only limitation is high cosmic opacity, which can prevent observations of the most distant galaxies. Hypothetically, it is possible to observe galaxies from the previous cycle/cycles, if their distance is higher than that corresponding to $z_{\max} \approx 14 - 15$. The identification of galaxies from the previous cycles will be, however, difficult, because their redshift will be a periodic function with increasing distance.

Obviously, a role of recycling processes is much more important in the cyclic cosmological model than in the Big Bang theory. The processes of formation/destruction of galaxies and their interaction with the circumgalactic medium through galactic winds and outflows (Muzahid et al. 2015; Hatch 2016; Segers et al. 2016; Anglés-Alcázar et al. 2017; Muratov et al. 2017; Brennan et al. 2018) should play a central role in this model. Similarly, the formation of metals in nuclear fusion should be balanced in the long term by their destruction invoked, for example, by quasars. Indications supporting that such a scenario is not ruled out are provided by studies of metallicity with cosmic time, when observations do not show convincing evidence of the metallicity evolution. By contrast, they indicate (Rauch 1998; Pettini 2004; Meiksin 2009) a widespread metal pollution of the intergalactic medium in all epochs of the Universe and a failure to detect a pristine material with no metals at high redshifts.

In summary, the opaque universe model and the Big Bang theory are completely different concepts of the Universe. Both theories successfully predict basic astronomical observations such as the universe expansion, the luminosity density evolution with redshift, the global stellar mass history, the SNe Ia measurements and the CMB observations. However, the Big Bang theory needs the existence of dark matter and dark energy, which are supported by no firm evidence. Moreover, they contradict small-scale observations in galaxies (Kroupa 2012, 2015; Buchert et al. 2016; Bullock & Boylan-Kolchin 2017) and are disfavoured by observations of gravitational waves (Ezquiaga & Zumalacárregui 2017). By contrast, the model of the eternal cyclic universe with high-redshift opacity is based on the standard physics, it is less speculative and predicts the current observations comparably well with no free parameters such as dark energy or dark matter. Nevertheless, this model opens other fundamental questions, such as about recycling processes of stars, galaxies and other objects in the Universe or about similarity/dissimilarity of individual cycles.

Acknowledgements

I thank very much for constructive and fruitful comments and suggestions of the Editor and three

anonymous referees.

A. Considering light-matter interactions in Einstein equations of general relativity

The Einstein field equations read

$$G^{\mu\nu} + \Lambda g^{\mu\nu} = \frac{8\pi G}{c^4} T^{\mu\nu}. \quad (\text{A1})$$

where $G^{\mu\nu}$ is the Einstein tensor, Λ is the cosmological constant, $g^{\mu\nu}$ is the metric tensor, G is the gravitational constant, c is the speed of light, and $T^{\mu\nu}$ is the energy-momentum tensor. The Einstein tensor $G^{\mu\nu}$ describes the curvature of the spacetime associated with gravity produced by the presence of matter and/or energy described by the energy-momentum tensor $T^{\mu\nu}$.

Since $G^{\mu\nu}_{;\nu} = 0$ and $g^{\mu\nu}_{;\nu} = 0$, we get

$$T^{\mu\nu}_{;\nu} = 0, \quad (\text{A2})$$

which expresses the energy-momentum conservation law.

The cosmological constant Λ in Eq. (A1) represents a non-gravitational field acting against the gravity. It was inserted into the equations by Einstein (1917) in order to maintain the Universe to be static. Since the physical nature of Λ was unclear, Einstein assumed the cosmological term in the simplest possible form. However, other forms of the cosmological term are, in principle, admissible. Obviously, the validity of the field equations (A1) is kept, if the cosmological term $\Lambda g^{\mu\nu}$ is substituted by the following more general term $\psi \Lambda^{\mu\nu}$,

$$G^{\mu\nu} + \psi \Lambda^{\mu\nu} = \frac{8\pi G}{c^4} T^{\mu\nu}, \quad (\text{A3})$$

where ψ is a constant, which should be determined, and $\Lambda^{\mu\nu}$ is the energy-momentum tensor of a non-gravitational field obeying the energy-momentum conservation law

$$\Lambda^{\mu\nu}_{;\nu} = 0. \quad (\text{A4})$$

In the next, tensor $\Lambda^{\mu\nu}$ in Eq. (A3) will be interpreted as the result of the light-matter interaction described in Section Light-matter interaction. The constant ψ standing at $\Lambda^{\mu\nu}$ in Eq. (A3) will be determined by applying the weak-field non-relativistic approximation, similarly as for determining the constant $8\pi G/c^4$ standing at the energy-momentum tensor $T^{\mu\nu}$.

Note that tensor $\Lambda^{\mu\nu}$ can formally be a part of the energy-momentum tensor $T^{\mu\nu}$. However, it is useful to treat it separately, in order to emphasize its non-gravitational nature similarly as done by Einstein in the case of the original cosmological constant Λ . In this way, tensor $T^{\mu\nu}$ is allocated for gravitational effects of mass and other physical fields only, but it does not reflect non-gravitational forces. Obviously, both approaches are mathematically equivalent, because if $\Lambda^{\mu\nu}$ is considered as a part of $T^{\mu\nu}$, matching the field equations for a weak non-relativistic field leads finally to decoupling of $\Lambda^{\mu\nu}$ and cancelling the factor $8\pi G/c^4$ standing at the term with $\Lambda^{\mu\nu}$.

For a perfect isotropic fluid, the energy-momentum tensor $T^{\mu\nu}$ reads

$$T^{\mu\nu} = \left(\rho + \frac{p}{c^2} \right) U^\mu U^\nu + p g^{\mu\nu}, \quad (\text{A5})$$

where ρ is the density, p is the pressure, and U^μ is the four velocity. In analogy to (A5), the isotropic cosmological tensor $\Lambda^{\mu\nu}$ can be described as

$$\Lambda^{\mu\nu} = \left(\rho_\Lambda + \frac{p_\Lambda}{c^2} \right) U^\mu U^\nu + p_\Lambda g^{\mu\nu}, \quad (\text{A6})$$

where ρ_Λ is the density, p_Λ is the pressure of the non-gravitational field produced by the light-matter interaction.

The unknown constant ψ in Eq. (A3) can now be found in a straightforward way assuming the weak-field approximation and using Eq. (16). This equation can be split into the Poisson equations for the gravitational potential Φ_G and for the potential of the light-matter interaction Φ_Λ as follows

$$\Delta \Phi_G = 4\pi G \rho, \quad (\text{A7})$$

$$\Delta\Phi_\Lambda = -\rho_\Lambda. \quad (\text{A8})$$

Taking into account that $\Lambda^{00} = \rho_\Lambda c^2$ and applying exactly the same procedure as when determining the constant $8\pi G/c^4$ standing at tensor $T^{\mu\nu}$ in Eq. (A1), we get $\psi = 2/c^4$. Hence, Eq. (A3) finally reads

$$G^{\mu\nu} + \frac{2}{c^4}\Lambda^{\mu\nu} = \frac{8\pi G}{c^4}T^{\mu\nu}. \quad (\text{A9})$$

Introducing the standard FLRW metric of the space defined by its Gaussian curvature k and by the scale factor $a(t)$ (Peacock 1999; Ryden 2016)

$$-c^2 d\tau^2 = -c^2 dt^2 + a^2(t) \left(\frac{dr^2}{1 - kr^2} + r^2 d\Omega^2 \right), \quad (\text{A10})$$

in Eqs. (A9), (A5) and (A6), we get a modified form of the Friedmann equations, which involve effects of the non-gravitational field $\Lambda^{\mu\nu}$

$$\left(\frac{\dot{a}}{a} \right)^2 = \frac{8\pi G}{3}\rho - \frac{2}{3}\rho_\Lambda - \frac{kc^2}{a^2}, \quad (\text{A11})$$

$$\frac{\ddot{a}}{a} = -\frac{4\pi G}{3} \left(\rho + \frac{3p}{c^2} \right) + \frac{1}{3} \left(\rho_\Lambda + \frac{3p_\Lambda}{c^2} \right). \quad (\text{A12})$$

Considering ρ and ρ_Λ depending on the scale factor $a(t)$ as $\rho = \rho_0 a^{-\alpha}$ and $\rho_\Lambda = \rho_{\Lambda 0} a^{-\beta}$, the equations of state for $T^{\mu\nu}$ and $\Lambda^{\mu\nu}$ yield

$$p = \frac{\alpha - 3}{3} c^2 \rho, \quad (\text{A13})$$

$$p_\Lambda = \frac{\beta - 3}{3} c^2 \rho_\Lambda, \quad (\text{A14})$$

and Eq. (A12) reads

$$\frac{\ddot{a}}{a} = -\frac{4\pi G}{3} (\alpha - 2) \rho + \frac{1}{3} (\beta - 2) \rho_\Lambda. \quad (\text{A15})$$

REFERENCES

- Abbott, B. P., Abbott, R., Abbott, T. D., et al. 2017, *Nature*, 551, 85
- Aguirre, A. 1999a, *ApJ*, 525, 583
- Aguirre, A. & Haiman, Z. 2000, *ApJ*, 532, 28
- Aguirre, A. N. 1999b, *ApJ*, 512, L19
- Aguirre, A. N. 2000, *ApJ*, 533, 1
- Anglés-Alcázar, D., Faucher-Giguère, C.-A., Kereš, D., et al. 2017, *MNRAS*, 470, 4698
- Bahcall, N. A., Lubin, L. M., & Dorman, V. 1995, *ApJ*, 447, L81
- Bernstein, R. A. 2007, *ApJ*, 666, 663
- Bernstein, R. A., Freedman, W. L., & Madore, B. F. 2002a, *ApJ*, 571, 56
- Bernstein, R. A., Freedman, W. L., & Madore, B. F. 2002b, *ApJ*, 571, 85
- Bernstein, R. A., Freedman, W. L., & Madore, B. F. 2002c, *ApJ*, 571, 107
- Bianchi, S. & Ferrara, A. 2005, *MNRAS*, 358, 379
- Bielby, R., Crighton, N. H. M., Fumagalli, M., et al. 2017, *MNRAS*, 468, 1373
- Birkinshaw, M. 1999, *Phys. Rep.*, 310, 97
- Blanton, M. R., Dalcanton, J., Eisenstein, D., et al. 2001, *AJ*, 121, 2358
- Blanton, M. R., Hogg, D. W., Bahcall, N. A., et al. 2003, *ApJ*, 592, 819
- Bohlin, R. C., Savage, B. D., & Drake, J. F. 1978, *ApJ*, 224, 132
- Bonamente, M., Joy, M. K., LaRoque, S. J., et al. 2006, *ApJ*, 647, 25
- Bond, H. E., Nelan, E. P., VandenBerg, D. A., Schaefer, G. H., & Harmer, D. 2013, *ApJ*, 765, L12
- Bond, J. R., Carr, B. J., & Hogan, C. J. 1991, *ApJ*, 367, 420
- Bonvin, V., Courbin, F., Suyu, S. H., et al. 2017, *MNRAS*, 465, 4914
- Bouwens, R. J., Bradley, L., Zitrin, A., et al. 2014a, *ApJ*, 795, 126
- Bouwens, R. J., Illingworth, G. D., Oesch, P. A., et al. 2014b, *ApJ*, 793, 115
- Brennan, R., Choi, E., Somerville, R. S., et al. 2018, *ApJ*, 860, 14
- Brown, W. R., Geller, M. J., Fabricant, D. G., & Kurtz, M. J. 2001, *AJ*, 122, 714
- Buchert, T., Coley, A. A., Kleinert, H., Roukema, B. F., & Wiltshire, D. L. 2016, *International Journal of Modern Physics D*, 25, 1630007
- Bullock, J. S. & Boylan-Kolchin, M. 2017, *Annual Review of Astronomy and Astrophysics*, 55, 343
- Calzetti, D. 2001, *PASP*, 113, 1449
- Calzetti, D., Armus, L., Bohlin, R. C., et al. 2000, *ApJ*, 533, 682
- Cardelli, J. A., Clayton, G. C., & Mathis, J. S. 1989, *ApJ*, 345, 245
- Carlstrom, J. E., Holder, G. P., & Reese, E. D. 2002, *Annual Review of Astronomy and Astrophysics*, 40, 643
- Chelouche, D., Koester, B. P., & Bowen, D. V. 2007, *ApJ*, 671, L97
- Clarkson, C., Cortès, M., & Bassett, B. 2007, *J. Cosmology Astropart. Phys.*, 2007, 011
- Cooray, A. 2016, *Royal Society Open Science*, 3, 150555
- Corasaniti, P. S. 2006, *MNRAS*, 372, 191
- Cross, N., Driver, S. P., Couch, W., et al. 2001, *MNRAS*, 324, 825
- Cruz, M., Martínez-González, E., Vielva, P., & Cayón, L. 2005, *MNRAS*, 356, 29
- Davies, J. I., Alton, P., Bianchi, S., & Trewella, M. 1998, *MNRAS*, 300, 1006
- Draine, B. T. 2003, *ARA&A*, 41, 241
- Draine, B. T. 2011, *Physics of the Interstellar and Intergalactic Medium*
- Draine, B. T. & Fraisse, A. A. 2009, *ApJ*, 696, 1

- Dwek, E. & Krennrich, F. 2005, *ApJ*, 618, 657
- Einstein, A. 1917, *Sitzungsberichte der Königlich Preußischen Akademie der Wissenschaften* (Berlin, 142
- Ellis, R. S., McLure, R. J., Dunlop, J. S., et al. 2013, *ApJ*, 763, L7
- Ezquiaga, J. M. & Zumalacárregui, M. 2017, *Phys. Rev. Lett.*, 119, 251304
- Fan, X., Strauss, M. A., Becker, R. H., et al. 2006, *AJ*, 132, 117
- Finkelman, I., Brosch, N., Kniazev, A. Y., et al. 2008, *MNRAS*, 390, 969
- Flynn, G. J. 1994, *Planet. Space Sci.*, 42, 1151
- Freedman, W. L., Madore, B. F., Gibson, B. K., et al. 2001, *ApJ*, 553, 47
- Freedman, W. L., Madore, B. F., Hatt, D., et al. 2019, *ApJ*, 882, 34
- Fujimoto, S., Ouchi, M., Ferrara, A., et al. 2019, *ApJ*, 887, 107
- Gilmore, R. C., Somerville, R. S., Primack, J. R., & Domínguez, A. 2012, *MNRAS*, 422, 3189
- Gold, B., Odegard, N., Weiland, J. L., et al. 2011, *ApJS*, 192, 15
- González, V., Labbé, I., Bouwens, R. J., et al. 2011, *ApJ*, 735, L34
- Hashimoto, T., Laporte, N., Mawatari, K., et al. 2018, *Nature*, 557, 392
- Hatch, N. 2016, *Science*, 354, 1102
- Hauser, M. G. & Dwek, E. 2001, *ARA&A*, 39, 249
- Hirashita, H. & Inoue, A. K. 2019, *MNRAS*, 487, 961
- Hoag, A., Bradač, M., Brammer, G., et al. 2018, *ApJ*, 854, 39
- Holwerda, B. W., Draine, B., Gordon, K. D., et al. 2007, *AJ*, 134, 2226
- Holwerda, B. W., Gonzalez, R. A., Allen, R. J., & van der Kruit, P. C. 2005, *AJ*, 129, 1381
- Hopkins, P. F., Quataert, E., & Murray, N. 2012, *MNRAS*, 421, 3522
- Howlett, C. & Davis, T. M. 2020, *MNRAS*, 492, 3803
- Ichiki, K. 2014, *Progress of Theoretical and Experimental Physics*, 2014, 06B109
- Jackson, N. 2015, *Living Reviews in Relativity*, 18, 2
- Jones, A. P., Tielens, A. G. G. M., & Hollenbach, D. J. 1996, *ApJ*, 469, 740
- Kajisawa, M., Ichikawa, T., Tanaka, I., et al. 2009, *ApJ*, 702, 1393
- Kippenhahn, R., Weigert, A., & Weiss, A. 2012, *Stellar Structure and Evolution*
- Kneiske, T. M., Bretz, T., Mannheim, K., & Hartmann, D. H. 2004, *A&A*, 413, 807
- Kocifaj, M., Kapisinsky, I., & Kundracik, F. 1999, *J. Quant. Spec. Radiat. Transf.*, 63, 1
- Kohout, T., Kallonen, A., Suuronen, J. P., et al. 2014, *Meteoritics and Planetary Science*, 49, 1157
- Kroupa, P. 2012, *Publications of the Astronomical Society of Australia*, 29, 395
- Kroupa, P. 2015, *Canadian Journal of Physics*, 93, 169
- Lagache, G., Puget, J.-L., & Dole, H. 2005, *ARA&A*, 43, 727
- Laporte, N., Ellis, R. S., Boone, F., et al. 2017, *ApJ*, 837, L21
- Lazarian, A. & Prunet, S. 2002, in *American Institute of Physics Conference Series*, Vol. 609, *Astrophysical Polarized Backgrounds*, ed. S. Cecchini, S. Cortiglioni, R. Sault, & C. Sbarra, 32–43
- Lee, K.-S., Ferguson, H. C., Wiklind, T., et al. 2012, *ApJ*, 752, 66
- Li, Z., Wang, G.-J., Liao, K., & Zhu, Z.-H. 2016, *ApJ*, 833, 240
- Liao, K. 2019, *ApJ*, 885, 70

- Lisenfeld, U., Relaño, M., Vílchez, J., Battaner, E., & Hermelo, I. 2008, in IAU Symposium, Vol. 255, IAU Symposium, ed. L. K. Hunt, S. C. Madden, & R. Schneider, 260–264
- Madau, P. & Dickinson, M. 2014, *ARA&A*, 52, 415
- Madau, P. & Pozzetti, L. 2000, *MNRAS*, 312, L9
- Marchesini, D., van Dokkum, P. G., Förster Schreiber, N. M., et al. 2009, *ApJ*, 701, 1765
- Martin, C. L. 2005, *ApJ*, 621, 227
- Mathis, J. S. 1990, *ARA&A*, 28, 37
- Mathis, J. S., Ruml, W., & Nordsieck, K. H. 1977, *ApJ*, 217, 425
- McLure, R. J., Dunlop, J. S., Bowler, R. A. A., et al. 2013, *MNRAS*, 432, 2696
- Meiksin, A. A. 2009, *Reviews of Modern Physics*, 81, 1405
- Ménard, B. & Fukugita, M. 2012, *ApJ*, 754, 116
- Ménard, B., Kilbinger, M., & Scranton, R. 2010a, *MNRAS*, 406, 1815
- Ménard, B., Scranton, R., Fukugita, M., & Richards, G. 2010b, *MNRAS*, 405, 1025
- Muller, S., Wu, S.-Y., Hsieh, B.-C., et al. 2008, *ApJ*, 680, 975
- Muratov, A. L., Kereš, D., Faucher-Giguère, C.-A., et al. 2017, *MNRAS*, 468, 4170
- Muzahid, S., Kacprzak, G. G., Churchill, C. W., et al. 2015, *ApJ*, 811, 132
- Narlikar, J. V., Vishwakarma, R. G., Hajian, A., et al. 2003, *ApJ*, 585, 1
- Nicastro, F., Kaastra, J., Krongold, Y., et al. 2018, *Nature*, 558, 406
- Oesch, P. A., Bouwens, R. J., Illingworth, G. D., et al. 2014, *ApJ*, 786, 108
- Oesch, P. A., Bouwens, R. J., Illingworth, G. D., Labbé, I., & Stefanon, M. 2018, *ApJ*, 855, 105
- Oesch, P. A., Brammer, G., van Dokkum, P. G., et al. 2016, *ApJ*, 819, 129
- Peacock, J. A. 1999, *Cosmological Physics*
- Peek, J. E. G., Ménard, B., & Corrales, L. 2015, *ApJ*, 813, 7
- Penton, S. V., Stocke, J. T., & Shull, J. M. 2002, *ApJ*, 565, 720
- Pérez-González, P. G., Rieke, G. H., Villar, V., et al. 2008, *ApJ*, 675, 234
- Perlmutter, S., Aldering, G., Goldhaber, G., et al. 1999, *ApJ*, 517, 565
- Péroux, C., McMahon, R. G., Storrie-Lombardi, L. J., & Irwin, M. J. 2003, *MNRAS*, 346, 1103
- Pessa, I., Tejos, N., Barrientos, L. F., et al. 2018, *MNRAS*, 477, 2991
- Pettini, M. 2004, in *Cosmochemistry. The melting pot of the elements*, ed. C. Esteban, R. García López, A. Herrero, & F. Sánchez, 257–298
- Pettini, M., Madau, P., Bolte, M., et al. 2003, *ApJ*, 594, 695
- Planck Collaboration, Ade, P. A. R., Aghanim, N., et al. 2015, *A&A*, 576, A104
- Planck Collaboration, Ade, P. A. R., Aghanim, N., et al. 2014, *A&A*, 571, A24
- Planck Collaboration, Ade, P. A. R., Aghanim, N., et al. 2016a, *A&A*, 594, A13
- Planck Collaboration, Aghanim, N., Akrami, Y., et al. 2018, *arXiv e-prints*, arXiv:1807.06209
- Planck Collaboration, Aghanim, N., Ashdown, M., et al. 2016b, *A&A*, 596, A109
- Pozzetti, L., Bolzonella, M., Zucca, E., et al. 2010, *A&A*, 523, A13
- Primack, J. R., Domínguez, A., Gilmore, R. C., & Somerville, R. S. 2011, in *American Institute of Physics Conference Series*, Vol. 1381, American Institute of Physics Conference Series, ed. F. A. Aharonian, W. Hofmann, & F. M. Rieger, 72–83
- Prochaska, J. X. & Herbert-Fort, S. 2004, *PASP*, 116, 622
- Qi, J.-Z., Cao, S., Pan, Y., & Li, J. 2019, *Physics of the Dark Universe*, 26, 100338

- Rachford, B. L., Snow, T. P., Tumlinson, J., et al. 2002, *ApJ*, 577, 221
- Rao, S. M., Turnshek, D. A., & Nestor, D. B. 2006, *ApJ*, 636, 610
- Rauch, M. 1998, *ARA&A*, 36, 267
- Reddy, N., Dickinson, M., Elbaz, D., et al. 2012, *ApJ*, 744, 154
- Reddy, N. A. & Steidel, C. C. 2009, *ApJ*, 692, 778
- Riess, A. G., Casertano, S., Yuan, W., et al. 2018, *ApJ*, 861, 126
- Riess, A. G., Filippenko, A. V., Challis, P., et al. 1998, *AJ*, 116, 1009
- Riess, A. G., Macri, L., Casertano, S., et al. 2011, *ApJ*, 730, 119
- Riess, A. G., Macri, L. M., Hoffmann, S. L., et al. 2016, *ApJ*, 826, 56
- Ryan-Weber, E. V., Pettini, M., & Madau, P. 2006, *MNRAS*, 371, L78
- Ryden, B. 2016, *Introduction to Cosmology*
- Sakstein, J. & Jain, B. 2017, *Phys. Rev. Lett.*, 119, 251303
- Salmon, B., Coe, D., Bradley, L., et al. 2018, *ApJ*, 864, L22
- Schechter, P. 1976, *ApJ*, 203, 297
- Schimminovich, D., Ilbert, O., Arnouts, S., et al. 2005, *ApJ*, 619, L47
- Schlegel, D. J., Finkbeiner, D. P., & Davis, M. 1998, *ApJ*, 500, 525
- Segers, M. C., Crain, R. A., Schaye, J., et al. 2016, *MNRAS*, 456, 1235
- Songaila, A. 2001, *ApJ*, 561, L153
- Songaila, A. & Cowie, L. L. 2010, *ApJ*, 721, 1448
- Suyu, S. H., Auger, M. W., Hilbert, S., et al. 2013, *ApJ*, 766, 70
- Tejos, N., Morris, S. L., Crighton, N. H. M., et al. 2012, *MNRAS*, 425, 245
- Tejos, N., Morris, S. L., Finn, C. W., et al. 2014, *MNRAS*, 437, 2017
- Tumlinson, J., Peebles, M. S., & Werk, J. K. 2017, *ARA&A*, 55, 389
- Vavryčuk, V. 2017a, *MNRAS*, 470, L44
- Vavryčuk, V. 2017b, *MNRAS*, 465, 1532
- Vavryčuk, V. 2018, *MNRAS*, 478, 283
- Vavryčuk, V. 2019, *MNRAS*, 489, L63
- Vavryčuk, V. & Kroupa, P. 2020, *MNRAS*, 497, 378
- Venemans, B. P., Walter, F., Decarli, R., et al. 2017, *ApJ*, 851, L8
- Vielva, P., Martínez-González, E., Barreiro, R. B., Sanz, J. L., & Cayón, L. 2004, *ApJ*, 609, 22
- Vitale, S. & Chen, H.-Y. 2018, *Phys. Rev. Lett.*, 121, 021303
- Wakker, B. P., Hernandez, A. K., French, D. M., et al. 2015, *ApJ*, 814, 40
- Watson, D., Christensen, L., Knudsen, K. K., et al. 2015, *Nature*, 519, 327
- Wei, J.-J. & Wu, X.-F. 2017, *ApJ*, 838, 160
- Weinberg, D. H., Mortonson, M. J., Eisenstein, D. J., et al. 2013, *Phys. Rep.*, 530, 87
- Weingartner, J. C. & Draine, B. T. 2001, *ApJ*, 548, 296
- Wolfe, A. M., Gawiser, E., & Prochaska, J. X. 2005, *ARA&A*, 43, 861
- Wright, E. L. 1982, *ApJ*, 255, 401
- Wright, E. L. 1987, *ApJ*, 320, 818
- Xie, X., Shao, Z., Shen, S., Liu, H., & Li, L. 2016, *ApJ*, 824, 38
- Xie, X., Shen, S., Shao, Z., & Yin, J. 2015, *ApJ*, 802, L16
- Yabe, K., Ohta, K., Iwata, I., et al. 2009, *ApJ*, 693, 507
- Yu, H. & Wang, F. Y. 2016, *ApJ*, 828, 85

- Zavala, J. A., Michałowski, M. J., Aretxaga, I.,
et al. 2015, MNRAS, 453, L88
- Zinnecker, H. & Yorke, H. W. 2007, Annual Re-
view of Astronomy and Astrophysics, 45, 481
- Zwaan, M. A., van der Hulst, J. M., Briggs, F. H.,
Verheijen, M. A. W., & Ryan-Weber, E. V.
2005, MNRAS, 364, 1467